ELSEVIER

Ceramics International 33 (2007) 869–874

CERAMICS INTERNATIONAL

www.elsevier.com/locate/ceramint

High-temperature deformation behaviour of TiO_2-doped 8 mol.% Y_2O_3-stabilized ZrO_2 (8Y-CSZ) under tension and compression

Süleyman Tekeli [a,*], Tiandan Chen [b], Hitoshi Nagayama [c], Taketo Sakuma [d], Martha L. Mecartney [b]

[a] *Materials Division, Technical Education Faculty, Gazi University, 06500 Besevler-Ankara, Turkey*
[b] *Department of Chemical Engineering and Materials Science, University of California, Irvine, CA 92697-2575, USA*
[c] *Department of Advanced Materials Science, School of Frontier Science, The University of Tokyo, 5-1-5 Kashiwanodo, Kashiwa 227-8561, Japan*
[d] *National Institute for Academic Degrees and University Evaluation, 1-29-1 Gakuennishimachi, Kodaira 187-8587, Japan*

Received 31 October 2005; received in revised form 18 November 2005; accepted 2 January 2006
Available online 18 April 2006

Abstract

The effect of TiO_2 addition on the phase stability of 8 mol.% yttria-stabilized cubic zirconia (8Y-CSZ) was investigated. XRD results showed that when the TiO_2 amount was less than 5 wt.%, the specimens were entirely single cubic phase; further addition of TiO_2 (5 wt.% or more) destabilized cubic zirconia phase and caused the formation of tetragonal phase. The amount of tetragonal phase increased with increasing TiO_2 content in the 8Y-CSZ matrix. The high-temperature deformation behavior of TiO_2-doped 8Y-CSZ was also studied under both tension and compression. The stress exponent and the activation energy values for 10 wt.% TiO_2-doped 8Y-CSZ were found to be 1 and 340 kJ/mol, respectively, using strain rate data from compression tests. The microstructure after and prior deformation was investigated using TEM. The grain shape remained equiaxed after extensive deformation but a high degree of residual stress developed. Under tension the addition of TiO_2 vastly decreased the flow stress for 8Y-CSZ and increased elongation to failure. The maximum elongation for 10 wt.% TiO_2-doped 8Y-CSZ was 203% at 1400 °C and at an initial strain rate of $1.3 \times 10^{-4}\ s^{-1}$ with a flow stress of 8 MPa, indicating the superplastic nature of this material.

Keywords: 8Y-CSZ; TiO_2 dopant; Microstructure; High-temperature creep; Tension and compression tests

1. Introduction

Superplasticity in ceramics was first reported in 3 mol.% yttria-stabilized tetragonal zirconia (3Y-TZP) by Wakai et al. [1] and extensive advances have been achieved using this material due to its grain size stability during high-temperature deformation [2]. Although the crystal structure of 8 mol.% yttria-stabilized cubic zirconia (8Y-CSZ) is close to that of 3Y-TZP [3], the elongation to failure for 8Y-CSZ is very limited (20%) due to strain hardening from both static and dynamic grain growth during high-temperature deformation [4].

To improve tensile ductility in cubic zirconia, attempts have been made using dopants and second phase dispersions, such as CuO [4], SiO_2 [5,6], CaO–TiO_2 [7] and Al_2O_3 [8]. Among them, SiO_2 and Al_2O_3 additives achieved more than 500% deformation [8]. The enhancement of ductility is due to limited grain growth through the addition of SiO_2 and Al_2O_3 intergranular phases. Recently, it has been reported that the addition of TiO_2 in solid solution in 8Y-CSZ can also vastly improve the tensile ductility [9]. It is interesting to note that the addition of TiO_2 is reported to promote grain growth, unlike the SiO_2 and Al_2O_3 dopants, which limit the grain growth. Previously Sakuma and Tsurui [10] had reported similar behavior for 3Y-TZP. Tensile ductility in 3Y-TZP was enhanced and flow stresses decreased with TiO_2 additions, even though the resultant grain size was larger than in undoped 3Y-TZP.

TiO_2-doped cubic zirconia is not only a superplastic ceramic, but also a potential candidate for a solid oxide fuel cell electrolyte because of its excellent stability at high temperature, good compatibility with the YSZ electrolytes, mixed conductivity and electrocatalytic activity [11]. Complex

* Corresponding author. Tel.: +90 312 4399760; fax: +90 312 2120059.
E-mail address: stekeli@gazi.edu.tr (S. Tekeli).

0272-8842/$32.00
doi:10.1016/j.ceramint.2006.01.014

shapes for fuel cell application with a higher efficiency could be net-shape formed using superplastic technology. This paper reports the microstructural evolution during deformation and creep behavior under compression for 8Y-CSZ doped with TiO_2 in an attempt to further explain the role of TiO_2.

2. Experimental procedures

Starting powders were nanoscale 8 mol.% yttria-stabilized cubic zirconia (Tosoh, Japan) and high-purity TiO_2 (Rare Metallic, Japan) powders. 8Y-CSZ powders were doped by adding different amounts of TiO_2 (up to 10 wt.%) and then ball-milling in ethanol for 24 h by using zirconia balls. The as-prepared slurries were dried in air and then die-pressed into cylinders and bars by uniaxial pressing at 40 MPa in a steel die followed by cold isostatic pressing at 100 MPa. The green compacts of the mixed powders were sintered at 1450 °C for an hour in air. Both compression and tensile tests were employed to investigate the creep behavior of different amount of TiO_2-doped 8Y-CSZ. The specimens used for compression tests were cylinders in 2 mm diameter and 5 mm height. The ends of each specimen were well-polished to make them parallel. To further decrease the friction between the specimen and SiC platens, the SiC platens were polished before each test and BN powder was put on the ends of the specimens. The furnace was heated to the test temperature within 3 h and then held there for 10 min to reach the equilibrium state before the test. The displacement of the specimen during deformation was monitored by an extensometer attached to the pushing rod. The load was adjusted to keep the true stress constant according to the increase of cross-area, which was determined from the displacement. The instantaneous true strain rate was calculated from the profiles of displacement dependence of time.

For tensile tests, specimens 2 mm × 2 mm in cross-section and 13.5 mm in gauge length were cut and ground from sintered bars. High-temperature tensile tests were carried out at a strain rate of $1.3 \times 10^{-4}\ s^{-1}$ and at a temperature of 1400 °C in air using an Instron type mechanical testing machine (Shimadzu Ag-5000C) equipped with a high-temperature furnace and SiC jigs. The high-temperature tensile test was started after 10 min holding. The testing temperature was measured by a Pt-PtRh thermocouple attached to a specimen.

The microstructure of as-sintered and deformed specimens was investigated using scanning electron microscopy (SEM) (Philips XL 30FEG) and transmission electron microscopy (TEM) (Philips CM20). Grain sizes were determined from the SEM micrographs using Scionimage software. The 3-d grain size was determined to be $1.56L$, where L is the average 2-d grain size measured from SEM images. TEM foils were prepared using conventional way, dimple polishing on one side, and ion beam thinning of both sides to electron transparency. To prevent charging problem, a few nanometers thick carbon film was deposited on the TEM sample. X-ray diffraction patterns (XRD) of the specimens were obtained using a Siemens D-5000 Diffractometer and monochromated high intensity Cu Kα radiation. A scan speed of 0.02 2θ/s was employed.

3. Results and discussion

3.1. XRD and SEM results

To determine the effect of TiO_2 addition on the crystal structure of 8Y-CSZ, XRD analysis was conducted on 8Y-CSZ specimens containing various amount of TiO_2 addition. Fig. 1 shows typical XRD patterns of undoped 8Y-CSZ and 8Y-CSZ with 0.5–10 wt.% TiO_2 sintered at 1450 °C. XRD analysis of the specimens containing up to 5 wt.% TiO_2 revealed only cubic fluorite reflections. However, when the TiO_2 concentration increased to 5 wt.% or more, the XRD results showed some small peaks indicating the formation of a tetragonal phase besides cubic fluorite phase. Therefore, the addition of more than 5 wt.% TiO_2 destabilized the cubic phase and induced the formation of the tetragonal phase. However, even when the TiO_2 concentration was 10 wt.%, no peaks from either TiO_2 or $TiZrO_4$ phases were observed.

SEM micrographs showed that the grain boundaries for undoped specimen were fairly regular, whereas the 5 and more wt.% TiO_2-doped specimens developed more irregular grain boundaries with a large number of small grains present at grain junctions and grain boundaries, indicating that the grain growth of the large grains was inhibited by the small grains during sintering. EDS analysis indicated that the small grains were tetragonal zirconia (Y-TZP), consistent with the XRD patterns (Fig. 1).

A comparison of the grain size of 8Y-CSZ specimens with TiO_2 content showed that grain size increased with increasing TiO_2 content up to 1 wt.% but further increases in TiO_2 resulted in a decreased grain size. The addition of 5 and more wt.% TiO_2 effectively limited the cubic grain growth by the pinning presence of small tetragonal grains.

3.2. Tensile deformation

In Fig. 1 the stress–strain curves for TiO_2-doped 8Y-CSZ are shown in comparison with previously published undoped 8Y-CSZ data from Yoshida et al.'s work [9]. Undoped 8Y-CSZ demonstrated an apparent strain hardening, a high flow stress of

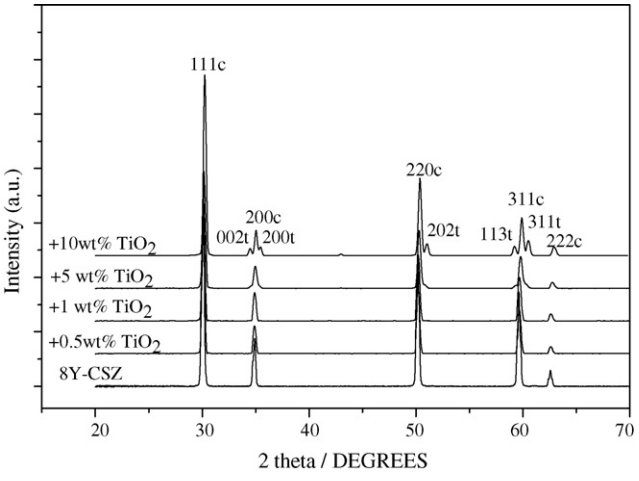

Fig. 1. X-ray diffraction patterns for undoped and TiO_2-doped 8Y-CSZ.

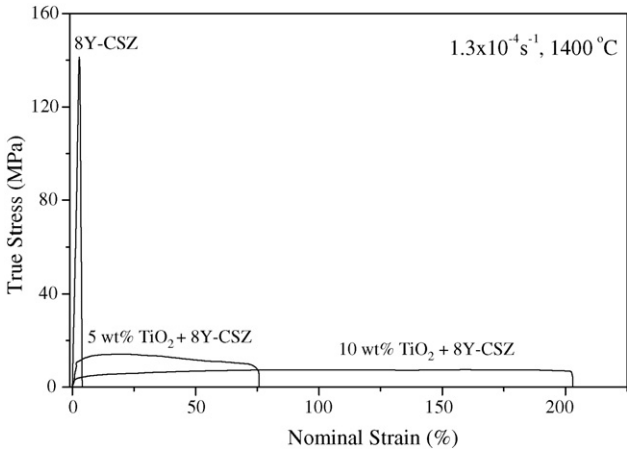

Fig. 2. Stress–strain curves for undoped 8Y-CSZ and TiO_2-doped 8Y-CSZ at 1400 °C and an initial strain rate of 1.3×10^{-4} s^{-1} under tension. Undoped 8Y-CSZ data is from reference [9].

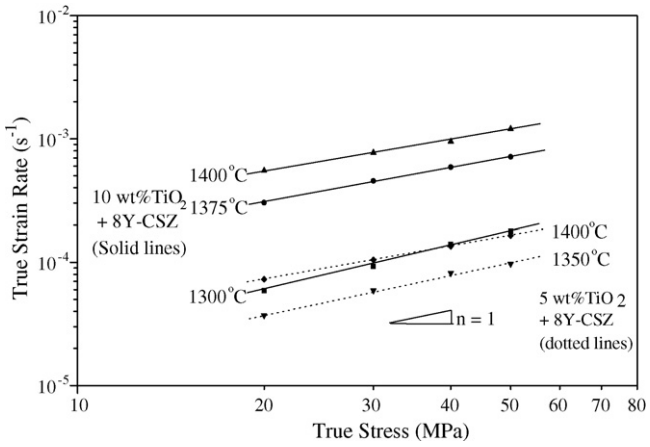

Fig. 4. True strain rate–stress relationship for 5 and 10 wt.% TiO_2-doped 8Y-CSZ deformed at various temperatures under compression.

about 140 MPa and a limited strain failure of about 4%. With the addition of 5 wt.% TiO_2, the flow curve showed a slight strain hardening at the beginning followed by a strain-softening region, when the flow stress decreased with tensile straining. For 10 wt.% TiO_2-doped 8Y-CSZ, however, specimen showed superplastic-like flow without apparent strain hardening or softening and the flow stress remained almost constant. With TiO_2 additions, the flow stress was significantly decreased. The maximum flow stress was about 14 MPa for 5 wt.% TiO_2-doped 8Y-CSZ and further decreased to 8 MPa for 10 wt.% TiO_2-doped 8Y-CSZ. Also the TiO_2 addition vastly improved the elongation to failure of 8Y-CSZ. As shown in Fig. 2, 5 and 10 wt.% TiO_2-doped 8Y-CSZ demonstrated an elongation to failure of 75 and 203% under tension, respectively.

3.3. Compressive deformation

Fig. 3 shows the true strain rate dependence with respect to true strain for 5 and 10 wt.% TiO_2-doped 8Y-CSZ deformed at 1300 °C under a constant compressive stress of 20 MPa. Both specimens demonstrated a decreased strain rate with increasing strain. The strain rate of 10 wt.% TiO_2-doped 8Y-CSZ was almost five times higher than that of 5 wt.% TiO_2-doped 8Y-CSZ.

Using data from different stress experiments under compression, the relationship between flow stress and strain rate is plotted on a logarithmic scale in Fig. 4 for the temperature range from 1300 to 1400 °C for 5 and 10 wt.% TiO_2-doped 8Y-CSZs. The plotted data points were the strain rates taken at a strain of 15%. The stress exponent was calculated from the slope lines. Both 5 and 10 wt.% TiO_2-doped 8Y-CSZs demonstrated a stress exponent close to 1 in the temperature range from 1300 to 1400 °C.

The temperature dependence of the strain rate for 10 wt.% TiO_2-doped 8Y-CSZ is shown in Fig. 5, where the true strain rates at 20 and 30 MPa were plotted against reciprocal absolute temperature. The deformation activation energy calculated from the slope is about 340 kJ/mol for 10 wt.% TiO_2-doped 8Y-CSZ.

3.4. TEM observations of microstructure changes

Representative TEM micrographs for 10 wt.% TiO_2-doped 8Y-CSZ in as-sintered and deformed states are shown in Fig. 6.

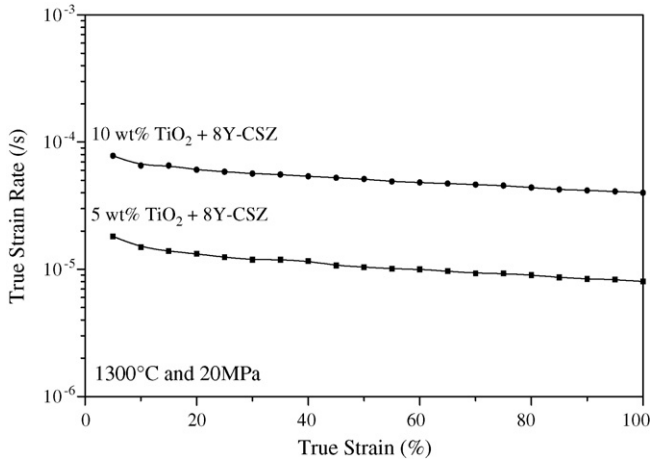

Fig. 3. True strain–strain rate curves in 5 and 10 wt.% TiO_2-doped 8Y-CSZ at 1300 °C and 20 MPa under compression.

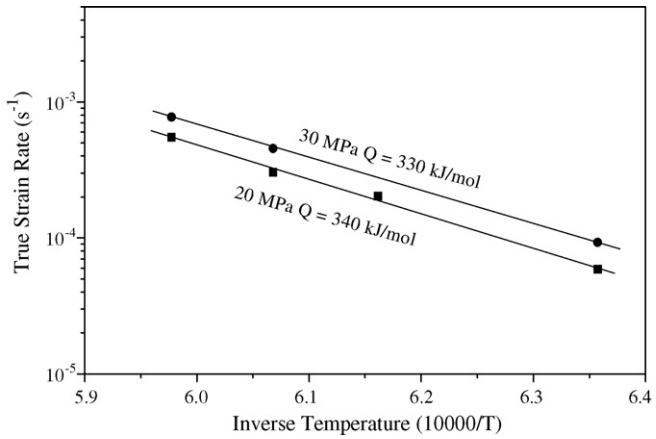

Fig. 5. Temperature dependence of true strain rate for 10 wt.% TiO_2-doped 8Y-CSZ under different compressive stresses.

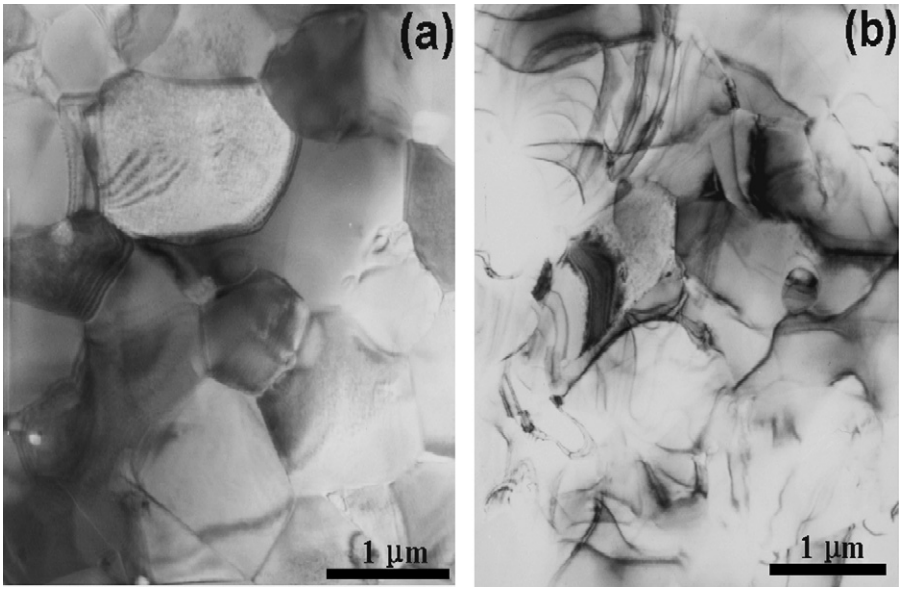

Fig. 6. TEM micrographs for (a) as-sintered and (b) 100% deformed 10 wt.% TiO_2-doped 8Y-CSZ specimens. Note the large amount of strain contrast after deformation.

Before deformation, the grains are mainly equiaxed and no grain boundary amorphous phase or glassy pockets at junctions were observed in conventional electron microscopy (Fig. 6 (a) and (b)). The microstructure for 10 wt.% TiO_2-doped 8Y-CSZ consisted of large and small grains. EDS analysis showed that the yttria concentration is much higher in large grains than that in small grains, and the titania solution in zirconia depends on yttria concentration in the yttria–zirconia solid solution and slightly higher in large grains. Before deformation, few isolated dislocations were observed. After deformation there is a large number of bend contours, which did not exist in the as-sintered materials, suggesting a high amount of residual strain in these specimens. These strain contrast and bend contours made the recognition of grain boundaries difficult in some regions. In spite of this, further investigation showed that the grains were still equiaxed after the extensive deformation and no apparent texture was developed during deformation. It is clear that the grain size after deformation is not significantly larger than that before deformation. No high density of dislocations was observed because the presence of strain contrast and bend contours.

4. Discussion

4.1. Creep parameters

The strain rate versus stress relationship in superplastic ceramics is usually expressed by the following semiempirical equation:

$$\dot{\varepsilon} = A\frac{\sigma^n}{d^p}\exp\left(\frac{-Q}{RT}\right) \quad (1)$$

where $\dot{\varepsilon}$ is the strain rate, A a constant, σ the flow stress, n the stress exponent, d the grain size, p the inverse grain size exponent, Q the activation energy, R the gas constant and T the absolute temperature.

From the above equation, under the constant stress and temperature, the decrease of strain rate should be due to dynamic grain growth during high-temperature deformation. Therefore, the decrease of strain rate with increasing strains in Fig. 3 indicates the occurrence of dynamic grain growth during the high-temperature deformation for both 5 and 10 wt.% TiO_2-doped 8Y-CSZ. Careful inspection of the strain rate–strain profiles in Fig. 3 shows that the decrease of strain rate for 5 wt.% TiO_2-doped 8Y-CSZ is slightly greater than that in 10 wt.% TiO_2-doped 8Y-CSZ, due to the higher percentage of tetragonal zirconia, which prevents grain growth in the latter. The grain growth in tetragonal zirconia is much more sluggish than that of cubic zirconia and the small tetragonal zirconia grains at junctions/boundaries hinder the grain growth of cubic zirconia matrix.

The stress exponents for 5 and 10 wt.% TiO_2-doped 8Y-CSZ under compression were calculated to around 1 (Fig. 4). A stress exponent of 1 is in the lower end of the reported values for 8Y-CSZ composites in the literature [5,6,8,12,13]. The stress exponent for single phase 8Y-CSZ deformed under tension was reported to be 2.5 by Tekeli and Davis [12]. Under compression tests, a stress exponent of about 2 at stress region less than 100 MPa and >5 (at higher stresses) was reported by Sudhir and Chokshi [13]. The addition of other dopants to 8Y-CSZ has been known to decrease the stress exponent. For example, the stress exponent for 5 wt.% SiO_2-doped 8Y-CSZ and 10 wt.% Al_2O_3-doped 8Y-CSZ was in the range of 1.3–1.7 [5,6] and 1.7–2.1 [8], respectively. The addition of TiO_2 further decreased the stress exponent down to a range of 1.1–1.3 under tension tests, which is similar to the stress exponent yielded from Fig. 4, i.e., in a range of 0.9–1.2 under compression.

The temperature dependence of the strain rate for 10 wt.% TiO_2-doped 8Y-CSZ is plotted against reciprocal absolute

temperature in Fig. 5. The deformation activation energy calculated from the slope was about 340 kJ/mol for 10 wt.% TiO_2-doped 8Y-CSZ. This value was lower than that reported for many 8Y-CSZ composites. The activation energy Q values for undoped 8Y-CSZ are reported to be 510 ± 40 kJ/mol [12] under tension tests and 430 ± 130 kJ/mol [13] under compression, respectively. The addition of TiO_2 decreased the activation energy to be about 360 kJ/mol, estimated from tensile tests data [9]. The above analysis also suggests that the stress exponent and activation energy values for 10 wt.% TiO_2-doped 8Y-CSZ determined under both tension and compression are very similar.

4.2. Flow stress and elongation

From Eq. (1), at a given strain rate, the flow stress should be proportional to the grain size and decrease with decreasing grain size. However, the flow stress reduction with 5 and 10 wt.% TiO_2 additions cannot be explained entirely by grain size. The maximum flow stress for undoped 8Y-CSZ with a grain size of 2.7 μm is about 140 MPa at 1400 °C with an initial strain rate of 1.3×10^{-4}. The measured average grain size for 5 wt.% TiO_2-doped 8Y-CSZ is 1.6 μm. Given a stress exponent of 1, assuming the grain size exponent to be either 2 or 3, the flow stress estimated from Eq. (1) for 5 wt.% TiO_2-doped 8Y-CSZ should be about 50 or 29 MPa, both of which are higher than the measured maximum flow stress of 14 MPa. In the work of Yoshida et al. [9] it was found that the flow stress in tension for 5 mol.% TiO_2-doped 8Y-CSZ with a larger grain size of 4.5 μm was even significantly lower than that of 8Y-CSZ with a grain size of 2.8 μm. Therefore, the flow stress is also affected by factors other than the average grain size. Those factors include grain shape, grain boundary structure/chemistry, and in particular, grain boundary chemical bonding state [14,15]. For instance, Yoshida et al. [15] studied the effect of 0.1 mol.% different cation dopants on the high-temperature creep resistance of alumina. They found that the dopants segregated at grain boundary and thus changed the boundary chemistry. The effect of dopant cations on the flow stress was correlated with the change in ionic bonding strength between the Al and O due to both a change in vacancy concentration and in covalent/ionic character. The enhancement of creep rate in Al_2O_3 by Ti dopants was reported to be due primarily to the reduction of ionicity. In the case of TiO_2-doped ZrO_2, the substitution of Zr^{4+} by Ti^{4+} causes a decrease in ionicity while the vacancy concentration should remain the same. A simple model using electronegativity values predicts that TiO_2-doped ZrO_2 will be more covalent than ZrO_2.

The enhancement of elongation to failure is often related to the decrease of flow stress. For instance, the improvement of the tensile ductility for TiO_2-doped TZP was attributed to the decrease of flow stress by Tsurui and Sakuma [10], in spite of the resultant grain growth due to the TiO_2 addition. The achievement of extensive elongation in SiO_2 doped tetragonal was explained by the combination of hindrance of grain growth by the intergranular silica phase and the decrease of flow stress [6]. In spite of that, the enhancement of elongation to failure cannot be explained solely by the decrease of flow stress. In the TZP (2.5 mol.% yttria), the elongations to failure increase with decreasing flow stress and increasing temperature. However, the elongation to failure for 5 wt.% TiO_2-doped TZP at 1500 °C is less than that at 1400 °C in spite of the lower flow stress at 1500 °C [10]. In another reference, Sakuma et al. [14] reported that the codoping 2 wt.% Al_2O_3 into 5 wt.% SiO_2-doped TZP further lowers the flow stress, but the elongation decreased to 220 from 1100% in 5 wt.% SiO_2-doped TZP [14]. Notice of the huge difference in ductility, they ascribed the difference is due to the changes of the grain boundary chemical bonding state.

4.3. Deformation mechanism

In spite of the extensive achievement that has been made since the first report of superplasticity in 3Y-TZP ceramics [1], there is no unambiguous deformation mechanism for superplasticity accepted in ceramics. More often than not, the deformation mechanism was identified by comparing the measured creep parameters, including n, p and Q with theoretical models together with the microstructural observations. Due to the stress exponent close to 1 in 15 mol.% TiO_2-doped 8Y-CSZ, Yoshida et al. [9] ascribed the deformation mechanism to diffusional creep. In the present work, after extensive 100% deformation of TiO_2-doped 8Y-CSZ under compression, grains remained equiaxed and no texture developed after deformation, which makes it unlikely that the diffusion creep is the main deformation mechanism for this material. In addition, there is large number of bend contours and strain contrast after deformation. Gust et al. [16] also reported the appearance of bend contours in deformed undoped 3Y-TZP, but not in glassy phase doped 3Y-TZP. They explained that the absence of bend contours is due to the fact that the doped glassy phase helps to relax the stresses during the deformation. It is likely that the bend contours were formed due to the stress concentration accumulated from the preceding grain boundary sliding, which was generally accepted as the main deformation mechanism in fine-grained ceramics. Direct evidence of grain boundary sliding has been observed using SEM [17]. Therefore, the main deformation mechanism for TiO_2-doped 8Y-CSZ is likely to be the grain boundary sliding accommodated by diffusion-related process.

5. Conclusion

TiO_2-doped cubic zirconia was prepared from nanoscale high-purity TiO_2 and 8 mol.% yttria-stabilized cubic zirconia powders. The phase and microstructural evolutions were investigated using XRD, SEM, TEM and EDS. XRD patterns found that the doped TiO_2 (up to 10 wt.%) was dissolved in the zirconia matrix and more than 5 wt.% TiO_2 dopant induced the formation of tetragonal zirconia in 8Y-CSZ. SEM observations showed that less than 1 wt.% TiO_2 dopant promoted the grain growth for 8Y-CSZ and further addition effectively limited the grain growth for cubic zirconia matrix due to the induced small tetragonal zirconia grains which act as pinning particles. The deformation behavior of TiO_2-doped cubic zirconia was investigated under both tension and compression tests. The

stress exponent and activation energy for 10 wt.% TiO_2-doped 8Y-CSZ was estimated to be about 1 and 340 kJ/mol from the strain rate data collected from compression tests. The addition of TiO_2 greatly decreased the flow stresses for the 8Y-CSZ and increased its elongation to failure under tension tests. In particular, the maximum elongation for 10 wt.% TiO_2-doped 8Y-CSZ was 203% at 1400 °C with an initial strain rate of $1.3 \times 10^{-4}\ s^{-1}$.

Acknowledgements

This research work is supported by DPT (the State Planning Organization of Turkey) under project number 2003K120470-18 and by the Division of Materials Research of the National Science Foundation (USA) under Grant No. 0207197.

References

[1] F. Wakai, S. Sagaguchi, Y. Matsuno, Adv. Ceram. Mater. 1 (1986) 259–263.
[2] K. Kajihara, Y. Yoshizawa, T. Sakuma, Acta. Metall. Mater. 43 (1995) 1235–1242.
[3] U. Messerschmidt, D. Baither, B. Baufeld, M. Bartsch, Mater. Sci. Eng. A 233 (1997) 61–74.
[4] S. Tekeli, T.J. Davies, Mater. Sci. Technol. 17 (2001) 109–112.
[5] A.A. Sharif, M.L. Mecartney, Acta. Mater. 51 (2003) 1633–1639.
[6] R.P. Dillon, S.S. Sosa, M.L. Mecartney, Scripta Mater. 50 (2004) 1441–1444.
[7] Y. Kitano, K. Yamada, E. Tanabe, M. Oka, K. Nagao, J. Electron. Microsc. 51 (Suppl.) (2002) s135–s141.
[8] A.A. Sharif, M.L. Mecartney, J. Eur. Ceram. Soc. 24 (2004) 2041–2047.
[9] H. Yoshida, A. Kubo, H. Ito, H. Nagayama, T. Sakuma, Scripta Mater. 52 (2005) 365–368.
[10] K. Tsurui, T. Sakuma, Scripta Mater. 34 (1996) 443–447.
[11] M.T. Colomer, J.R. Jurado, J. Solid State Chem. 165 (2002) 79–88.
[12] S. Tekeli, T.J. Davies, Mater. Sci. Eng. A. 297 (2001) 168–175.
[13] B. Sudhir, A.H. Chokshi, J. Am. Ceram. Soc. 84 (2001) 2625–2632.
[14] T. Sakuma, Y. Ikuhara, Y. Takigawa, P. Thavorniti, Mater. Sci. Eng. A 234–236 (1997) 226–229.
[15] H. Yoshida, Y. Ikuhara, T. Sakuma, Acta. Mater. 50 (2002) 2955–2966.
[16] M. Gust, G. Goo, J. Wolfenstine, M.L. Mecartney, J. Am. Ceram. Soc. 76 (1993) 1681–1690.
[17] R. Duclos, J. Eur. Ceram. Soc. 24 (2004) 3103–3110.